



Performance of chip-scale optical frequency comb generators in coherent WDM communications

PABLO MARIN-PALOMO,^{1,4}  JUNED N. KEMAL,¹  TOBIAS J. KIPPENBERG,² WOLFGANG FREUDE,¹  SEBASTIAN RANDEL,¹ AND CHRISTIAN KOOS^{1,3,5} 

¹*Institute of Photonics and Quantum Electronics (IPQ), Karlsruhe Institute of Technology (KIT), 76131 Karlsruhe, Germany*

²*Laboratory of Photonics and Quantum Measurements (LPQM), École Polytechnique Fédérale de Lausanne (EPFL), Lausanne, Switzerland*

³*Institute of Microstructure Technology (IMT), Karlsruhe Institute of Technology (KIT), 76344 Eggenstein-Leopoldshafen, Germany*

⁴*pablo.marin@kit.edu*

⁵*christian.koos@kit.edu*

Abstract: Optical frequency combs have the potential to become key building blocks of wavelength-division multiplexing (WDM) communication systems. The strictly equidistant narrow-band spectral lines of a frequency comb can serve either as carriers for parallel WDM transmission or as local-oscillator (LO) tones for parallel coherent reception. When it comes to highly scalable WDM transceivers with compact form factor, chip-scale comb sources are of particular interest, and recent experiments have demonstrated the viability of such devices for high-speed communications with line rates of tens of Tbit/s. However, the output power of chip-scale comb sources is generally lower than that of their conventional discrete-element counterparts, thus requiring additional amplifiers and impairing the optical signal-to-noise ratio (OSNR). In this paper, we investigate the influence of the power and optical carrier-to-noise ratio (OCNR) of the comb lines on the performance of the WDM link. We identify two distinctively different regimes, where the transmission performance is either limited by the comb source or by the link and the associated in-line amplifiers. We further investigate the impact of line-to-line power variations on the achievable OSNR and link capacity using a soliton Kerr frequency comb as a particularly interesting example. We believe that our findings will help to compare different comb generator types and to benchmark them with respect to the achievable transmission performance.

© 2020 Optical Society of America under the terms of the [OSA Open Access Publishing Agreement](#)

1. Introduction

Frequency comb generators (FCG) have emerged as light sources for wavelength-division multiplexing (WDM) communications [1–10]. A frequency comb consists of a multitude of inherently equidistant spectral lines, hence relaxing the requirements for inter-channel guard bands and avoiding individual frequency control of each line as needed in conventional schemes that use arrays of independent lasers. This advantage also applies to the WDM receiver, where an array of discrete local oscillators (LO) might be replaced by a single FCG [5,9,10]. Using an LO comb for parallel coherent reception of WDM signals further facilitates joint digital signal processing of the channels and can thus reduce receiver complexity and increase phase-noise tolerance [11,12]. Moreover, parallel coherent reception with frequency-locked LO tones might even allow to reconstruct the time-domain waveform of the overall WDM signal and thus permit compensation of impairments caused by optical nonlinearities of the transmission fiber [13].

Among the various FCG concepts, chip-scale devices are of particular interest [4–9,14–19]. Combined with advanced photonic integrated circuits for modulation, multiplexing, routing, and reception of data signals, chip-scale FCG offer a path towards highly scalable, compact and energy-efficient WDM transceivers that can offer multi-terabit transmission capacities per fiber. However, chip-scale FCG are also subject to specific limitations when compared to arrays of individual tunable lasers [20] or to discrete-element comb generators that rely, e.g., on highly nonlinear optical fibers [1–3]. In particular, the tones of a chip-scale FCG usually feature comparatively low optical power, in some cases combined with limited optical carrier-to-noise ratio (OCNR). For large line counts, optical amplifiers are then needed to boost the optical power prior to modulation, which might further decrease the OCNR. In addition, comb lines generated by chip-scale devices may exhibit pronounced spectral power variations and thus often require spectral flattening, which can lead to further degradation of the optical signal-to-noise ratio (OSNR). However, while these aspects can lead to severe performance limitations, a quantitative analysis of the impact of OCNR limitations and line-to-line power variations on the transmission performance of comb-based WDM transceivers is still lacking.

In this paper, we formulate a model that allows to estimate the transmission performance of comb-based WDM systems under the influence of OCNR limitations and line-to-line power variations. Our model builds upon previous studies of WDM systems in general [21] and of comb-based WDM transmission [11] and extends them to quantify the OSNR at the receiver of the WDM link for different comb-source parameters and transmission distances. We identify two distinctively different operation regimes for such links: For low line powers or low OCNR levels, the transmission performance is limited by the comb source and the associated amplifiers, whereas the in-line amplifiers along the link turn out to be the main limitation for high line powers and high OCNR. We further investigate the impact of line-to-line power variations on the performance of the WDM link. To this end, we use a soliton Kerr frequency comb generator as an example of a comb source that offers a large number of narrowband tones [22]. We also analyze the achievable capacity as a function of the link distance for a soliton Kerr frequency comb. For metropolitan-area links of up to 400 km, our model predicts capacities of around 80 Tbit/s. We believe that our findings will help to broadly compare and benchmark different chip-scale comb generator concepts with respect to achievable transmission performance in a given use case.

This paper is structured as follows: In Section 2, we introduce the model of the comb-based transmission link that represents the base of our investigation. Section 3 describes the results of this investigation and formulates requirements with respect to comb-line power and OCNR that should be fulfilled by chip-scale comb generators to ensure link-limited transmission. Section 4 is dedicated to investigating the impact of spectral flattening.

2. OSNR limitations in a comb-based WDM system

In comb-based WDM systems, one of the main aspects leading to limited transmission performance is the fact that the overall output power of the comb source is limited and that spectral splitting of the comb lines leads to additional optical loss. This may lead to low powers per line, which often requires additional amplifiers to boost the power prior to modulation, thereby decreasing the OCNR of the lines entering the modulator array. In the following, we analyze these effects and quantify their impact on the overall transmission performance.

The performance of a WDM link is often described by the OSNR measured at the receiver input. The OSNR is defined as the ratio of the signal power to the amplified spontaneous emission (ASE) noise power within a reference bandwidth $B_{\text{ref}} = 12.5$ GHz, corresponding to a reference wavelength span of 0.1 nm at a center wavelength of 1.55 μm . The OSNR can be translated into the signal-to-noise ratio (SNR) that refers to the actual bandwidth of a specific signal [23]. For a

coherent system limited by ASE noise,

$$SNR = \frac{2B_{\text{ref}}}{pR_s} \text{OSNR}, \quad (1)$$

where R_s is the symbol rate, $p = 1$ for a single polarization signal and $p = 2$ for a polarization-multiplexed signal [23]. In the following, we will consider polarization-multiplexed signals.

In a comb-based WDM system, the OSNR of a WDM channel will depend on the comb line power P_{line} and the OCNR of the comb line, $\text{OCNR}_{\text{line}}$. In analogy to the OSNR, the OCNR relates the comb line power to the power of the background noise, measured again within a reference bandwidth B_{ref} centered at the comb line frequency. The sum of the noise power in both polarizations at the output of the FCG is given by

$$P_{\text{noise}} = N_0 B_{\text{ref}} = \frac{P_{\text{line}}}{\text{OCNR}_{\text{line}}}. \quad (2)$$

Here, N_0 is the noise spectral power density. Thus, P_{line} and $\text{OCNR}_{\text{line}}$ impact the OSNR of a WDM channel and can limit the achievable spectral efficiency for a given reach. Note that we disregard the impact of the optical linewidth in our analysis. The linewidth of the individual comb lines is not altered by the link and it only becomes relevant after the channel is coherently detected. At the receiver, the channels are analyzed individually and the linewidth may be treated as the property of an individual carrier tone rather than as a frequency comb property. The associated limitations have been discussed in the literature for different modulation formats and can be readily applied to frequency-comb transmission [12,24].

For a quantitative analysis, consider the WDM link depicted in Fig. 1 consisting of a WDM transmitter, a link with M fiber spans, and a WDM receiver [11]. Note that the comb line powers P_{line} of most chip-scale FCG are usually much weaker than the power levels emitted by state-of-the-art continuous-wave laser diodes used in conventional WDM systems. For practical transmission systems, it is therefore necessary to amplify the comb lines prior to modulation by sending them through a dedicated optical amplifier with gain $G_0 > 1$. Data are encoded onto the various carriers by a WDM modulation unit comprising a WDM demultiplexer (DEMUX), an array of dual-polarization in-phase/quadrature (I/Q) modulators, and a WDM multiplexer (MUX). The power transmission factor of the WDM modulation unit is denoted as $g_0 < 1$ and accounts for the insertion losses of the multiplexer and the demultiplexer as well as for the insertion and modulation losses of the I/Q modulators. In our analysis we consider the bandwidth of the WDM DEMUX filter to be equal to the line spacing of the frequency comb. It can, however, be advantageous to reduce the filter bandwidth in order to suppress unwanted additive noise between the carriers. Note that the modulator will act as a polarizer and thus only the noise co-polarized with the laser carrier is considered. The signal and noise power at the output of the WDM modulation unit are given by

$$P_{\text{signal}}^{(0)} = g_0 G_0 P_{\text{line}}, \quad P_{\text{noise}}^{(0)} = \frac{g_0}{2} \left[\underbrace{G_0 N_0 B_{\text{ref}}}_{\text{amplified OFC noise}} + \underbrace{F_0 h f (G_0 - 1) B_{\text{ref}}}_{\text{ASE noise of comb amplifier}} \right]. \quad (3)$$

In these relations, F_0 is the noise figure of the comb amplifier, and hf is the photon energy [21]. For simplicity, we consider a frequency comb with equal power P_{line} for each spectral line, in Section 4, we investigate the impact of line-to-line power variations. Note that in our analysis, the noise is considered to be stationary, i.e., we do not account for any modulation of the noise contributions of the comb source and the comb amplifier. In the typically used link-limited regime, the effect of modulated noise can be disregarded since the stationary ASE noise added in the link dominates. In the source-limited regime, neglecting the amplitude modulation of the noise might lead to a slight overestimation of the performance.

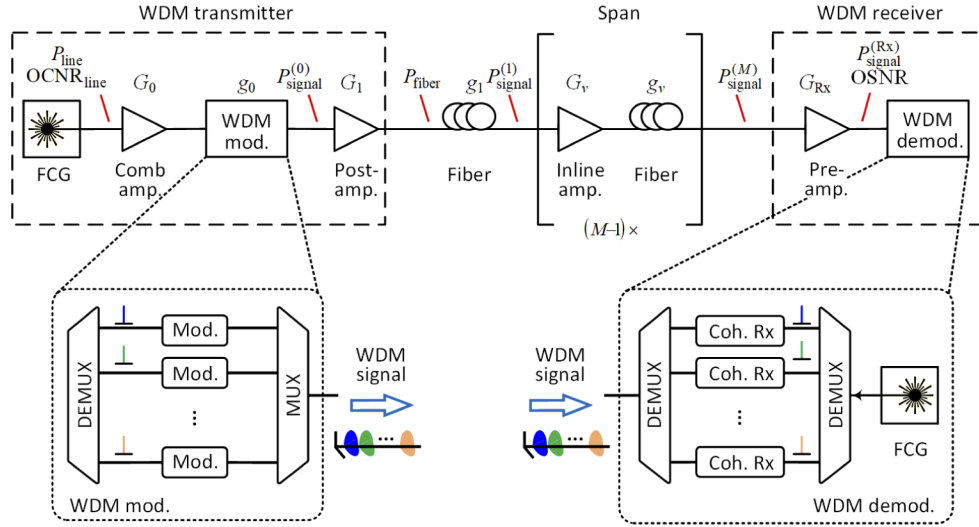


Fig. 1. Schematic of a comb-based WDM transmission and reception system. The tones of a chip-scale frequency comb generator (FCG) are first amplified by an optical amplifier (Comb amp.) before data are encoded on each line in the WDM modulation unit (WDM mod.), which comprises a WDM demultiplexer (DEMUX), an array of dual-polarization I/Q modulators (Mod.), and a WDM multiplexer (MUX). The polarization multiplexed WDM signal is then boosted by an optical amplifier (Post-amp.) and transmitted through the fiber link consisting of at least one span. Each of the $M - 1$ additional spans contains an in-line amplifier (In-line amp.) which compensates the loss of the corresponding fiber section. The data from each WDM channel are recovered at the WDM receiver, which contains a pre-amplifier (Pre-amp.) and a WDM demodulation unit (WDM demod.). The WDM demodulation unit uses a multitude of LO tones derived from a second FCG.

The polarization-multiplexed WDM signal is then boosted by a post-amplifier with gain G_1 and launched into the first fiber section, which attenuates the power by $g_1 < 1$,

$$P_{\text{signal}}^{(1)} = g_1 G_1 P_{\text{signal}}^{(0)}, \quad P_{\text{noise}}^{(1)} = g_1 [G_1 P_{\text{noise}}^{(0)} + F_1 h f (G_1 - 1) B_{\text{ref}}]. \quad (4)$$

The first fiber span may be followed by $M - 1$ additional fiber sections, each attenuating the power by $g_m < 1$ and by the same number of additional in-line amplifiers with gain G_m .

These in-line amplifiers are used to compensate the loss of the respective fiber section such that $G_m g_m = 1$, $m = 2 \dots M$. Setting $G_m = G$, and $F_m = F$ for $m = 2 \dots M$, and $g_m = g$ for $m = 1 \dots M$, the signal power and the noise power after the transmission link are given as

$$P_{\text{signal}}^{(M)} = P_{\text{signal}}^{(1)}, \quad P_{\text{noise}}^{(M)} = P_{\text{noise}}^{(1)} + g(M - 1) F h f (G - 1) B_{\text{ref}}. \quad (5)$$

The data from each WDM channel are recovered at the WDM receiver, which contains an optical pre-amplifier with gain G_{Rx} and noise figure F_{Rx} and a WDM demodulation unit. The WDM demodulation unit uses a multitude of LO tones derived from a second FCG to recover the transmitted data with an array of IQ detectors. The signal power and the noise power at the output of the pre-amplifier are given by

$$P_{\text{signal}}^{(\text{Rx})} = G_{\text{Rx}} P_{\text{signal}}^{(M)}, \quad P_{\text{noise}}^{(\text{Rx})} = G_{\text{Rx}} P_{\text{noise}}^{(M)} + F_{\text{Rx}} h f (G_{\text{Rx}} - 1) B_{\text{ref}}. \quad (6)$$

To obtain the OSNR for a single WDM channel, the ratio of the received signal power and the noise power in the reference bandwidth B_{ref} needs to be calculated,

$$\text{OSNR} = \frac{P_{\text{signal}}^{(\text{Rx})}}{P_{\text{noise}}^{(\text{Rx})}}. \quad (7)$$

Introducing Eqs. (3)–(6) into Eq. (7) for a given line power P_{line} and $\text{OCNR}_{\text{line}}$ the OSNR per channel can be expressed as

$$\text{OSNR} = \frac{g_0 G_0 P_{\text{line}}}{\underbrace{\frac{g_0 G_0 P_{\text{line}}}{2 \text{OCNR}_{\text{line}}}}_{\text{ampl. FCG noise}} + \underbrace{hf B_{\text{ref}} \left(\frac{g_0}{2} (G_0 - 1) F_0 + \frac{G_1 - 1}{G_1} F_1 + (M - 1) \frac{G - 1}{G_1} F + \frac{G_{\text{Rx}} - 1}{G_{\text{Rx}} g G_1} F_{\text{Rx}} \right)}_{\text{amplifier noise}}}. \quad (8)$$

Note that for a high number of spans, i.e., $M \gg 1$, the noise of the receiver pre-amplifier does not play a role any more, since the noise background is dominated by the noise contribution from the various amplifiers along the link.

In Section 3, we apply Eq. (8) to a comb-based WDM system to derive the OSNR as a function of the line power P_{line} and the number M of fiber spans, see Fig. 2. In this analysis, we assume a spectrally flat comb where all tones have the same power. In addition, the gain G_1 of the post-amplifier is assumed to be the same as the gain G of the in-line amplifiers, and the gain G_0 of the comb amplifier is adjusted such that a launch power into each fiber section of $P_{\text{fiber}} = 0$ dBm is reached after the post-amplifier. This launch power is commonly used in 32 GBd WDM links for keeping the nonlinear impairments low while maintaining high OSNR levels [25,26]. In Section 4, we expand this consideration and analyze the more practical case where P_{line} varies from line to line. In this case, the resulting OSNR will depend on the comb line. As an example of a chip-scale FCG with large line count, we investigate a soliton Kerr comb generated in an integrated optical microresonator [5,6,22] and consider the OSNR variations from line to line as a function of P_{line} and $\text{OCNR}_{\text{line}}$, see Fig. 3. In this analysis, we set the G_0 such that a fixed output power of 25 dBm is obtained, and we adjust G_1 such that $P_{\text{fiber}} = 0$ dBm.

3. OSNR limitations considering frequency combs with flat spectra

In this section, we make use of Eq. (8) to estimate the OSNR as a function of P_{line} and $\text{OCNR}_{\text{line}}$ for different numbers M of fiber spans, see Fig. 2. The various parameters used for this study are specified in Table 1. For the WDM modulation unit, an overall insertion loss of 25 dB is assumed, comprising 3.5 dB of insertion loss each for the WDM demultiplexer and the multiplexer [27], 13 dB of loss for the dual-polarization IQ modulators [28], and an additional 5 dB of modulation loss, which are assumed to be independent of the modulation format for simplicity. Note that the results shown in Fig. 2 do not change significantly when varying these losses by a few dB while compensating the variation by an adjustment of the gain G_0 of the comb amplifier. The fiber spans are assumed to feature a power loss of 15 dB each, corresponding to 75 km of single-mode fiber with a propagation loss of 0.2 dB/km. The power loss of each span is exactly compensated by the 15 dB gain of the corresponding in-line amplifier such that a signal launch power of $P_{\text{fiber}} = 0$ dBm per channel is maintained for all spans. For simplicity, the gain and the noise figure of the receiver pre-amplifier is assumed to be identical to that of the in-line amplifiers, leading to a signal power of 0 dBm per wavelength channel at the input of the receiver DEMUX. Figure 2(a) shows the OSNR as a function of P_{line} for various span counts M . The $\text{OCNR}_{\text{line}}$ of the comb lines is assumed to be infinite, i.e., the FCG itself does not introduce any practically relevant additive noise background. This can, e.g., be accomplished by soliton Kerr comb generators, see Fig. 3, where most of the comb lines do not contain relevant additive noise background. For low line

powers P_{line} , Fig. 2(a) shows that the noise level at the receiver is dominated by the contribution of the comb amplifier. As a consequence, the OSNR increases in proportion to P_{line} and is essentially independent of the span count M . In this regime, transmission performance is limited by the comb source and its associated amplifier (“source-limited”). For high comb line powers P_{line} , in contrast, the noise level at the receiver is dominated by the contributions of the various amplifiers along the link (“link-limited”). In this regime, the OSNR is essentially independent of P_{line} and decreases with each additional span. For a given number of spans, the transition between both regimes is indicated by black circles in Fig. 2(a), indicating the points where the OSNR has decreased by 1 dB in comparison to its limit at high line power P_{line} . When using frequency combs in WDM systems, operation in the link-limited regime is preferred. Depending on the number of spans, this requires a minimum comb line power between approximately -25 dBm and -15 dBm. Note that, in principle, the gain G_1 of the post amplifier could be decreased while increasing the gain G_0 of the comb amplifier. For source-limited transmission, the overall impact would be small since the OSNR is mainly dictated by the comparatively low line power P_{line} that enters the comb amplifier. For link-limited transmission over a small number of spans, the OSNR can be slightly improved by decreasing the gain G_1 and increasing the gain G_0 while maintaining power levels of about 10 dBm per line at the output of the comb amplifier. In our analysis, we assume equal noise figures of 5 dB for all optical amplifiers. This is a realistic assumption since gain values of the amplifiers do not differ considerably, even when considering additional measures for spectral flattening, see Table 2 in Section 4.

Table 1. Model parameters used for generating Figs. 2(a) and 2(b) from Eq. (8)^a

Variable	Description	Value	
B_{ref}	Reference bandwidth for OSNR and OCNR calculation	12.5 GHz	
$G_m P_{\text{signal}}^{(m)} = P_{\text{fiber}}$	Signal power per WDM channel at the input of each fiber span	1 mW	0 dBm
g_0	Power transmission factor of WDM modulation unit	3.2×10^{-3}	-25 dB
G_0	Power gain factor of comb amplifier	$P_{\text{fiber}} / (P_{\text{line}} g_0 G_1)$	
F_0	Noise figure of comb amplifier	3.2	5 dB
G_1	Power gain factor of post-amplifier	32	15 dB
F_1	Noise figure of post-amplifier	3.2	5 dB
$g_m = g$	Power transmission factor of fiber section	3.2×10^{-2}	-15 dB
$G_m = G = g^{-1}$	Power gain factor of post- and inline-amplifier	32	15 dB
$F_m = F$	Noise figure of post- and inline-amplifiers	3.2	5 dB
G_{Rx}	Power gain factor of pre-amplifier	32	15 dB
F_{Rx}	Noise figure of pre-amplifier	3.2	5 dB

^aThe fiber attenuation g_m , amplifier gain G_m , and noise figures F_m are assumed to be the same for all M fiber links denoted by subscript $m = 1 \dots M$. For the spectral flattening considered in Section 4, we adjust the power transmission factor g_0 of the WDM modulation unit or the gain G_0 individually for each channel, and we choose the gain G_1 of the post-amplifier to maintain a constant power per channel of 0 dBm at the input of the first fiber span. Specifically, for the variable-gain scenario, g_0 is varied such that $g_0 P_{\text{line}}$ is constant across all comb lines, whereas for the variable-gain scenario, G_0 is varied from channel to channel such that $G_0 P_{\text{line}}$ is constant.

Figure 2(a) can be used as a guide for estimating the performance requirements for comb sources in WDM applications. As a reference, the plot indicates the minimum OSNR required for transmission of a net data rate of 400 Gbit/s or 600 Gbit/s per WDM channel using 16QAM or 64QAM as a modulation format, respectively. In both cases, advanced forward-error correction (FEC) schemes with 11% overhead and a BER threshold of 1.2×10^{-2} [29] are assumed, requiring a symbol rate of 56 GBd to provide the specified net data rates. Note that we do not account for the format-dependent modulation losses, but assume an overall insertion loss of the modulator of

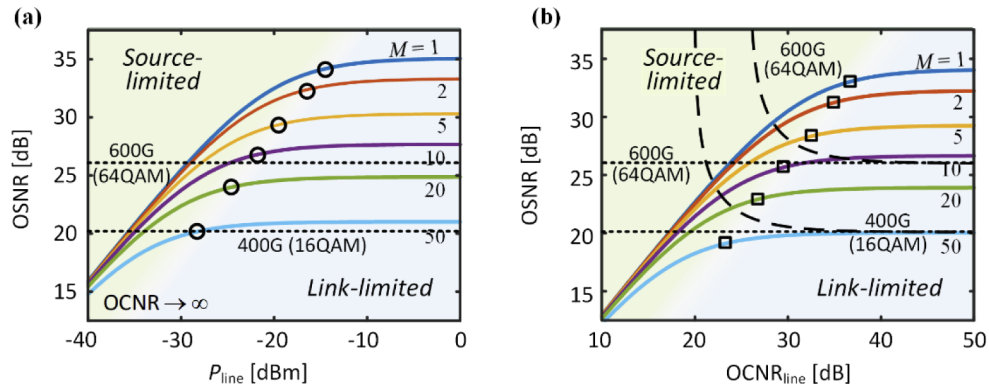


Fig. 2. Influence of the comb-line power P_{line} and of its carrier-to-noise ratio $\text{OCNR}_{\text{line}}$ on the achievable optical signal-to-noise ratio OSNR at the WDM receivers for different values M of 75 km-long spans with 0.2 dB/km loss, see Table 1 for the model parameters used. **(a)** OSNR as a function of P_{line} in the limit of a high $\text{OCNR}_{\text{line}}$. The plot reveals two regimes: For source-limited transmission at low line powers, the OSNR is dominated by the contribution of the comb amplifier, whereas the contributions of the various amplifiers along the link dominates for link-limited transmission at high line powers. The transition between both regimes is indicated by black circles which mark the points where the OSNR has decreased by 1 dB in comparison to its limit at high comb line powers. The dotted horizontal lines indicate the minimum OSNR required for transmission of a net data rate of 400 Gbit/s using 16QAM and of 600 Gbit/s using 64QAM as a modulation format [29]. **(b)** OSNR at the WDM receiver as a function of $\text{OCNR}_{\text{line}}$ for comb line powers P_{line} that correspond to the transition points marked by circles in (a). For low $\text{OCNR}_{\text{line}}$, OSNR is dominated by the noise of the comb source, and the transmission performance is source-limited. For high $\text{OCNR}_{\text{line}}$, the OSNR is independent of the $\text{OCNR}_{\text{line}}$ and the transmission performance is link-limited. The dotted horizontal lines indicate again the minimum OSNR required for transmission of a net data rate of 400 Gbit/s using 16QAM and of 600 Gbit/s using 64QAM as a modulation format, assuming an ideal LO comb with infinite $\text{OCNR}_{\text{line}}$. In case of a real LO comb with finite $\text{OCNR}_{\text{line}}$, the OSNR requirements for a given BER become more stringent when approaching the link-limited regime, see dashed lines, which were derived from Eq. (9).

25 dB both for 16QAM and 64QAM. This loss includes both the optical insertion loss of the device and the modulation loss.

For many practically relevant comb sources, the $\text{OCNR}_{\text{line}}$ is finite, which also impairs the transmission performance. Figure 2(b) shows the OSNR at the receiver as a function of $\text{OCNR}_{\text{line}}$ for various span counts M . In this plot, the comb line power is the minimum value required for link-limited transmission, as indicated by the corresponding transition points in Fig. 2(a). For low $\text{OCNR}_{\text{line}}$, the noise level at the receiver is dominated by the amplified noise background of the comb source, and the $\text{OCNR}_{\text{line}}$ and OSNR are essentially identical. In this case, the link performance is again source-limited. For high $\text{OCNR}_{\text{line}}$, the OSNR is dictated by the accumulated ASE noise of the post-amplifier and the in-line amplifiers and is thus independent of the $\text{OCNR}_{\text{line}}$. In this regime, the transmission performance is link-limited. Depending on the number of spans, the minimum $\text{OCNR}_{\text{line}}$ values needed for link-limited transmission range between approximately 25 dB and 35 dB. The transition between both regimes is marked by black squares in Fig. 2(b), indicating the points where the OSNR has decreased by 1 dB in comparison to its respective limit at high $\text{OCNR}_{\text{line}}$.

Note that finite OCNR can also become relevant at the receiver in case a frequency comb is used as multi-wavelength LO. In a simplified consideration, we may assume that the transmitter

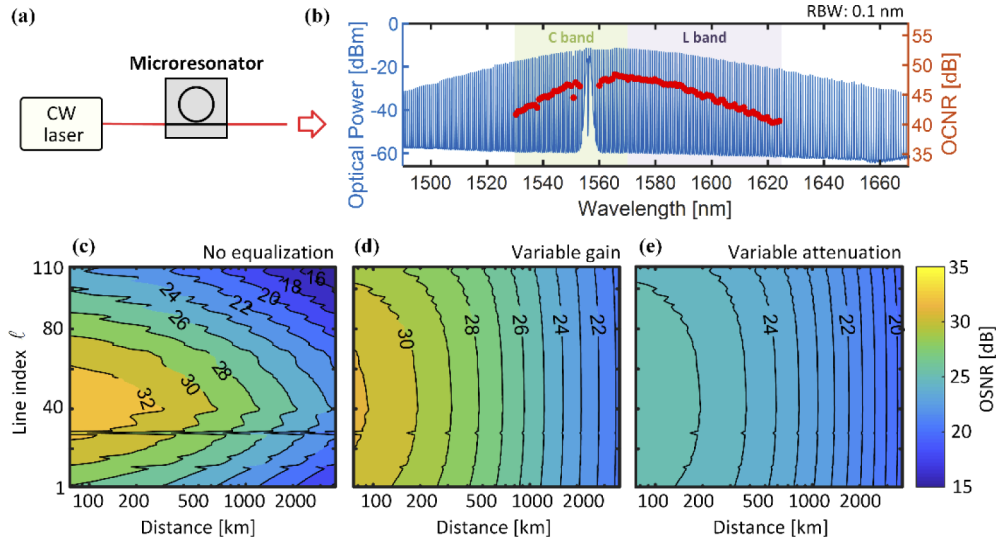


Fig. 3. Single-soliton Kerr frequency combs and impact of line-to-line P_{line} and $\text{OCNR}_{\text{line}}$ variations on the OSNR. (a) Kerr comb generation: A high- Q Kerr nonlinear microresonator is pumped by a CW laser. Under appropriate conditions, cascaded degenerate and non-degenerate four-wave mixing leads to formation of new spectral lines. For single-soliton states, the superposition of the phase-locked optical tones forms an ultra-short soliton pulse circulating in the cavity. This leads to a comb spectrum with a broadband envelope. (b) Spectrum of a single-soliton Kerr frequency comb generated in a SiN microresonator [5]. The comb offers 110 carriers in the telecommunication C and L band (1530 nm . . . 1625 nm), spaced by approximately 100 GHz. In the center of the spectrum, the comb line power amounts to -11 dBm, and the OCNr is approximately 48 dB. Towards the wings of the comb, both line power and OCNr decrease. (c-e) OSNR as a function of the link distance and the comb line index, ℓ , (c) without equalizing the power per line (“No equalization”); (d) equalizing the power per line by using a spectrally variable gain in first amplifier stage of Fig. 1 (“Variable gain”); (e) equalizing the power per line by introducing individual power attenuations for each channel (“Variable loss”) at the WDM modulation unit from Fig. 1.

and the receiver rely on comb sources with identical OCNr. In this case, the OCNr of the LO comb is always higher than the OSNR of the received signal, which is affected by the ASE noise of the post-amplifier at the transmitter, the pre-amplifier at the receiver and the inline amplifiers along the link. In the link-limited transmission regime, the noise accumulated along the link dominates, and the noise of the LO comb can hence be neglected. The only case for which the impact of LO noise becomes important is the source-limited transmission regime, i.e., the left-hand part of Fig. 2(b). In this region, the LO comb noise additionally impairs the reception, thereby increasing the OSNR of the data signal that is required for a given BER. This is indicated by the dashed lines for the 400 Gbit/s 16QAM signal and for the 600 Gbit/s 64QAM signal. Neglecting noise-noise beating in the coherent receiver and defining OSNR_{∞} as the OSNR required for a given BER in case of an ideal noise-less LO comb (dotted line in Fig. 2(b)), the OSNR in case of a non-ideal LO-comb with finite $\text{OCNR}_{\text{line}}$ can be expressed as

$$\text{OSNR} = \left(\frac{1}{\text{OSNR}_{\infty}} - \frac{1}{\text{OCNR}_{\text{line}}} \right)^{-1}. \quad (9)$$

Note that the underlying BER can only be achieved for $\text{OCNR}_{\text{line}} > \text{OSNR}_{\infty}$ and that the achievable OSNR is always worse than the $\text{OCNR}_{\text{line}}$ of the transmitter comb, i.e., $\text{OSNR} \leq \text{OCNR}_{\text{line}}$ if the transmitter and the receiver rely on comb generators with identical $\text{OCNR}_{\text{line}}$.

4. OSNR limitations considering frequency combs with line-to-line power variations

Chip-scale comb sources, relying on different comb generation approaches, have been used in a variety of WDM transmission experiments covering a wide range of data rates, channel counts, and line spacings [4–10,14–19]. In these WDM transmission experiments, the line to line variations of P_{line} and $\text{OCNR}_{\text{line}}$ lead to a channel-dependent OSNR. In the following, we will analyze the impact of line-to-line power variations on the transmission performance of the WDM link for different transmission distances. To this end, we consider a Kerr frequency comb generated in a silicon nitride (SiN) microresonator [22] as an illustrative example. Kerr frequency combs are generated by pumping a high- Q microresonator with a strong CW laser, see Fig. 3(a). Under appropriate pumping conditions, cascaded four-wave mixing leads to the formation of a multitude of spectral lines. As a technically attractive example, we consider so-called single-Kerr-soliton states, which rely on a double balance of parametric gain and cavity loss as well as second order dispersion and nonlinearity and which consist of a single ultra-short pulse circulating in the micro-resonator [21]. This leads to broadband frequency combs providing tens or even hundreds of high-quality tones for massively parallel WDM transmission [5]. Note that single-soliton Kerr combs are considered for illustrative purposes only and that other comb sources or other comb states in Kerr-nonlinear microresonators can also be used for WDM transmission. As an example, Turing rolls and dark solitons can achieve high power conversion efficiencies and have been used in WDM transmission [4,6]. However, the number of comb lines is rather limited and the line-to-line power variations may be strong. Solitons generated in microresonators with higher-order dispersion, such as quartic solitons [30], may provide frequency combs with broad and smooth spectra and might thus lend themselves to massively parallel WDM transmission.

Table 2. Model parameters for each WDM transmission scenario in Fig. 3 and Fig. 4^a

	No equalization	Variable gain	Variable attenuation
g_0	−25 dB	−25 dB	−35 dB . . . −25 dB
G_0	19 dB	16 dB . . . 26 dB	19 dB
G_1	21 dB	21 dB	27 dB

^aThe gain G_0 of the comb amplifier is adjusted to reach a fixed output power of 25 dBm fed into the WDM modulation unit, while the gain G_1 of the post-amplifier is adjusted to obtain a power per channel of 0 dBm at the input of the first fiber span. The quantity g_0 denotes the power transmission of the WDM modulation unit and of the associated variable attenuators used for spectral flattening.

An example of a measured single-soliton Kerr comb spectrum is shown in Fig. 3(b), which is measured after equalizing the residual pump power with a notch filter (not shown in Fig. 3). This spectrum comprises around 110 carriers spaced by approximately 100 GHz within the telecommunication C and L band (1530 nm . . . 1610 nm). The line powers range from −11 dBm near the center to −20 dBm at the edges of the telecommunication window, and the OCNR values range from 48 dB to 40 dB, which would safely permit link-limited transmission in realistic WDM systems, see Fig. 2. While the on-chip pump power used to generate the comb in the originally experiment was approximately 29 dBm, recent advances in fabrication technology and system design have shown the possibility to significantly reduce the required pump power for soliton generation and increase the power conversion efficiency, e.g., by increasing the quality factor of the microresonator [31] or incorporating the microresonator into the cavity of the pump

laser [32]. Using Eq. (8) with the P_{line} and $\text{OCNR}_{\text{line}}$ values measured from the carriers of the soliton frequency comb and with the model parameters from Table 1 and Table 2, we calculate the optical signal-to-noise ratio OSNR_ℓ , $\ell = 1 \dots L$, for each individual channel as a function of the link distance, see Figs. 3(c)–3(e). For this analysis, we assume an output power of 25 dBm provided by the comb amplifier, which corresponds to a power of approximately 5 dBm per line at the input of the WDM modulation unit. The gain of the post-amplifier is set such that a power per line of 0 dBm is launched into each fiber span.

We investigate three different WDM transmission scenarios, refer to Table 2 for the gain G_0 and G_1 of the comb amplifier and the post-amplifier for each of these scenarios as well as for the corresponding power transmission factor g_0 of the WDM modulation unit. In the first scenario, the comb lines are not equalized in power (“No equalization”), and all amplifiers are assumed to have a spectrally flat gain. Note that this scenario is typically not implemented in practical WDM transmission systems, and it is used here as a reference. In our analysis we assume the power $P_{\text{fiber}} = 0$ dBm to be the average signal power per WDM channel at the input of each fiber span. The individual per-channel launch powers vary from -7 dBm to 3 dBm. In the second scenario, the power per line is equalized at the first amplifier stage of Fig. 1 by using, e.g., a wavelength-dependent gain G_0 such that the comb lines at the edge of the telecommunication windows are amplified more than those at the center to reach a spectrally uniform per-channel launch power of 0 dBm into the first fiber span. This can be achieved, e.g., by adapting the gain profile of the optical amplifiers to the spectral variations of the frequency comb. For simplicity, we assume the noise figure of all amplifiers to be wavelength-independent. We refer to this scheme as variable-gain equalization (“Variable gain”). In the third scenario, the power per line is equalized at the WDM modulator stage of Fig. 1 by considering a channel dependent power transmission g_0 . This can, e.g., be accomplished by using optical attenuators or by adjusting the drive voltages of the IQ modulators, such that the channels at the center of the comb spectrum experience a higher attenuation. In this scenario, we assume again amplifiers with spectrally flat gain and noise figure. The gain G_1 of the post-amplifier is increased such that $P_{\text{fiber}} = 0$ dBm, we refer to this scheme as variable-loss equalization (“Variable loss”).

If no power equalization to the comb lines is performed, strong channel-to-channel OSNR variations can be observed for all transmission distances, see Fig. 3(c) “No equalization”. Note that these channel-dependent OSNR variations do not decrease with propagation distance since the amplifier noise term in Eq. (8) dominates the noise power in the denominator such that the difference in P_{line} at the output of the frequency comb will determine the OSNR_ℓ . If the comb line powers are equalized at the first amplification stage, see Fig. 3(d) “Variable gain”, all channels will exhibit the same OSNR_ℓ for large transmission distances. This can be understood by the fact that, at large distances, the accumulated ASE noise from the in-line amplifiers will dominate the noise power in all channels such that the initial OSNR differences become irrelevant. The same is true if the comb line powers are equalized at the WDM modulation stage, see Fig. 3(e) “Variable attenuation” – also here the accumulated ASE noise will dominate the noise power with increasing distance. In addition, the initial attenuation of the center channels will decrease the associated OSNR for short transmission distances, but this difference disappears for longer links as the accumulated ASE noise of the in-line amplifiers dominates. As a consequence, the performance of the second and the third transmission scenario converge with increasing transmission distance.

To quantitatively compare the transmission performance of the three different schemes, we estimate the maximum capacity for a given reach [33],

$$C = f_r \sum_{\ell=1}^L \log_2(1 + \text{SNR}_\ell), \quad (10)$$

where f_r is the comb line spacing, L is the number of comb lines, and SNR_ℓ is obtained from the OSNR_ℓ through Eq. (1) with a bandwidth $B = f_r$. Equation (9) considers the maximum capacity for each channel which can be theoretically achieved by using an arbitrarily complex modulation format [33]. The link capacity according to Eq. (10) for $f_r = 100$ GHz and $L = 110$, as well as the spectral efficiency, $\text{SE} = C / (Lf_r)$ are indicated as solid lines in Fig. 4. The line spacing was chosen to maximize the per-channel symbol rate while still being compatible with the bandwidth of available signal generators [34] and IQ modulators [35].

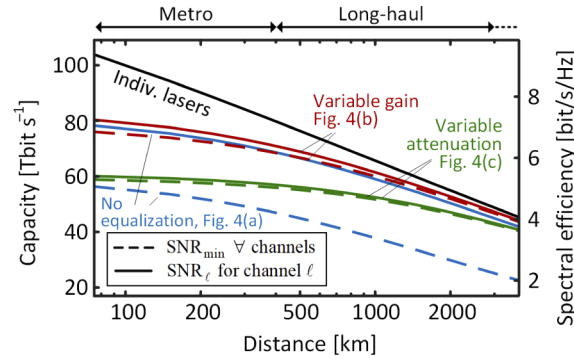


Fig. 4. Total capacity and spectral efficiency of a WDM transmission link using individual lasers (black line) single-soliton Kerr frequency combs with $L = 110$ comb lines and a comb line spacing $f_r = 100$ GHz (colored traces). Blue traces: No equalization done (“No equalization”). Red traces: Flattening of the frequency by spectrally variable gain in the first amplifying stage (“Variable gain”). Green trace: Flattening of the frequency comb by spectrally variable attenuation in the WDM modulation unit (“Variable attenuation”). Black trace: Individual lasers each with 13 dBm of optical power and 60 dB of OCNR. Solid lines: The capacity is optimized individually for each channel. Dashed lines: The per-channel capacity is derived from the smallest SNR, SNR_{\min} in the WDM link.

For Metro links, both the scheme without equalization (“No equalization”) and the scheme with spectrally variable gain (“Variable gain”) lead to a higher capacity than the scheme based on spectrally variable attenuation (“Variable attenuation”), offering link capacities of around 80 Tbit/s. For longer reach, the capacity decreases, and the differences between the three schemes become negligible. Note that our consideration does not account for the impact of fiber nonlinearity, which might lead to further limitations at longer transmission distances [36].

Another scenario of practical interest is the case where all modulators of the various WDM channels are operated with the same modulation format and same FEC overhead is applied to all channels. The maximum capacity is then dictated by the channel with the lowest SNR, SNR_{\min} , leading to

$$C = Lf_r \log_2(1 + \text{SNR}_{\min}). \quad (11)$$

The results of this consideration are indicated as dashed lines in Fig. 4. For metro links, the variable-gain scheme provides the highest SNR_{\min} and thus the highest capacity and spectral efficiency. For longer links, the performance of the variable-gain scheme approaches that of the variable-attenuation scheme. The capacity is then the same as the one obtained from Eq. (10). As a comparison, Fig. 4 also shows the case of using individual lasers instead of the carriers of a soliton Kerr frequency comb. For this analysis, we have assumed a fixed power per line of 13 dBm fed directly into the modulator along with an OCNR of 60 dB. For short transmission distances, the performance of the comb-based scheme is source limited due to the low power per line. The analysis also shows that the spectral flatness and the gain flattening technique have a

direct impact on the achievable capacity. For longer reach, all schemes with flat spectra approach the same link-limited performance.

Regarding technical realizations of chip-scale WDM transceivers, it should be noted that integration of high-power comb amplifiers might represent a challenge, in particular when it comes to massively parallel transmission with tens of even hundreds of comb lines [5,7]. For the example of an input power of approximately 3 mW per line measured at the input of the modulator, a high-power semiconductor optical amplifier (SOA) with a saturation output power of 23 dBm [37] could be used to handle approximately 70 lines. For bigger line counts or higher powers per line, the tones have to be amplified in separate groups or fiber amplifiers have to be used. For Kerr combs, another challenge might arise from the fact that the residual pump after the resonator may be much stronger than the other comb tones. Suppressing the pump leads to additional energy loss. Note, however, that in all of these cases, the power consumption of the comb generator and the comb amplifier is shared by all comb lines such that the power consumption per line still remains reasonable [5].

5. Summary

We have investigated the influence of the comb line power and optical carrier-to-noise ratio (OCNR) on the optical signal-to-noise ratio (OSNR) for comb-based WDM transmission systems. We identify two regimes of operation depending on whether the transmission performance is limited by the comb source (“source-limited”) or by the link and the associated in-line amplifiers (“link-limited”). Our analysis indicates that, depending on the number of spans, minimum comb line powers between -25 dBm and -15 dBm and minimum $\text{OCNR}_{\text{line}}$ values between 25 dB and 35 dB are needed for link-limited transmission. In addition, we investigated the impact of line-to-line power variations on the achievable OSNR and the overall link capacity for WDM system that relies on single-soliton Kerr frequency combs as a particularly interesting example. We find that OSNR levels of around 30 dB for Metro links lead to capacities of around 80 Tbit/s. We believe that our findings will help to broadly compare different comb generator types and to benchmark them with respect to the achievable transmission performance.

Funding

European Research Council (773248); Deutsche Forschungsgemeinschaft (258734477-SFB 1173, 403188360, SPP 2111); Erasmus Mundus Doctorate Programme Europhotonics (159224-1-2009-1-FR-ERA MUNDUS-EMJD); Alfried Krupp von Bohlen und Halbach-Stiftung; Helmholtz International Research School for Teratronics, Karlsruhe Institute of Technology; H2020 Marie Skłodowska-Curie Actions (812818).

Disclosures

The authors declare that there are no conflicts of interest related to this article.

References

1. V. Ataie, E. Temprana, L. Liu, E. Myslivets, B. P.-P. Kuo, N. Alic, and S. Radic, “Ultrahigh count coherent WDM channels transmission using optical parametric comb-based frequency synthesizer,” *J. Lightwave Technol.* **33**(3), 694–699 (2015).
2. B. J. Puttnam, R. S. Luís, W. Klaus, J. Sakaguchi, J.-M. Delgado Mendinueta, Y. Awaji, N. Wada, Y. Tamura, T. Hayashi, M. Hirano, and J. Marciante, “2.15 Pb/s transmission using a 22 core homogeneous single-mode multi-core fiber and wideband optical comb,” in *European Conference on Optical Communication (ECOC, 2015)*, paper PDP 3.1.
3. D. Hillerkuss, R. Schmogrow, M. Meyer, S. Wolf, M. Jordan, P. Kleinow, N. Lindenmann, P. C. Schindler, A. Melikyan, X. Yang, S. Ben-Ezra, B. Nebendahl, M. Dreschmann, J. Meyer, F. Parmigiani, P. Petropoulos, B. Resan, A. Oehler, K. Weingarten, L. Altenhain, T. Ellermeyer, M. Moeller, M. Huebner, J. Becker, C. Koos, W. Freude, and J. Leuthold, “Single-laser 32.5 Tbit/s Nyquist WDM transmission,” *J. Opt. Commun. Netw.* **4**(10), 715–723 (2012).

4. J. Pfeifle, V. Brasch, M. Laueremann, Y. Yu, D. Wegner, T. Herr, K. Hartinger, P. Schindler, J. Li, D. Hillerkuss, R. Schmogrow, C. Weimann, R. Holzwarth, W. Freude, J. Leuthold, T. Kippenberg, and C. Koos, "Coherent terabit communications with microresonator Kerr frequency combs," *Nat. Photonics* **8**(5), 375–380 (2014).
5. P. Marin-Palomo, J. N. Kemal, M. Karpov, A. Kordts, J. Pfeifle, M. H. P. Pfeiffer, P. Trocha, S. Wolf, V. Brasch, M. H. Anderson, R. Rosenberger, K. Vijayan, W. Freude, T. J. Kippenberg, and C. Koos, "Microresonator-based solitons for massively parallel coherent optical communications," *Nature* **546**(7657), 274–279 (2017).
6. A. Fülöp, M. Mazur, A. Lorences-Riesgo, O. B. Helgason, P.-H. Wang, Y. Xuan, D. E. Leaird, M. Qi, P. A. Andrekson, A. M. Weiner, and V. Torres-Company, "High-order coherent communications using mode-locked dark-pulse Kerr combs from microresonators," *Nat. Commun.* **9**(1), 1598 (2018).
7. H. Hu, F. Da Ros, M. Pu, F. Ye, K. Ingerslev, E. Porto da Silva, M. Nooruzzaman, Y. Amma, Y. Sasaki, T. Mizuno, Y. Miyamoto, L. Ottaviano, E. Semenova, P. Guan, D. Zibar, M. Galili, K. Yvind, T. Morioka, and L. K. Oxenløwe, "Single-source chip-based frequency comb enabling extreme parallel data transmission," *Nat. Photonics* **12**(8), 469–473 (2018).
8. J. Pfeifle, V. Vujicic, R. T. Watts, P. C. Schindler, C. Weimann, R. Zhou, W. Freude, L. P. Barry, and C. Koos, "Flexible terabit/s Nyquist-WDM super-channels using a gain-switched comb source," *Opt. Express* **23**(2), 724–738 (2015).
9. J. N. Kemal, J. Pfeifle, P. Marin-Palomo, M. D. G. Pascual, S. Wolf, F. Smyth, W. Freude, and C. Koos, "Multi-wavelength coherent transmission using an optical frequency comb as a local oscillator," *Opt. Express* **24**(22), 25432–25445 (2016).
10. J. N. Kemal, P. Marin-Palomo, V. Panapakkam, P. Trocha, S. Wolf, K. Merghem, F. Lelarge, A. Ramdane, S. Randel, W. Freude, and C. Koos, "Coherent WDM transmission using quantum-dash model-locked laser diodes as multi-wavelength source and local oscillator," *Opt. Express* (2019, in Press).
11. V. Torres-Company, J. Schröder, A. Fülöp, M. Mazur, L. Lundberg, O. B. Helgason, M. Karlsson, and P. A. Andrekson, "Laser frequency combs for coherent optical communications," *J. Lightwave Technol.* **37**(7), 1663–1670 (2019).
12. L. Lundberg, M. Karlsson, A. Lorences-Riesgo, M. Mazur, V. Torres-Company, J. Schröder, and P. A. Andrekson, "Frequency comb-based WDM transmission systems enabling joint signal processing," *Appl. Sci.* **8**(5), 718 (2018).
13. E. Temprana, E. Myslivets, B. P.-P. Kuo, L. Liu, V. Ataie, N. Alic, and S. Radic, "Overcoming Kerr-induced capacity limit in optical fiber transmission," *Science* **348**(6242), 1445–1448 (2015).
14. T. Shao, R. Zhou, V. Vujicic, M. D. Gutierrez Pascual, P. M. Anandarajah, and L. P. Barry, "100 km coherent Nyquist ultradense wavelength division multiplexed passive optical network using a tunable gain-switched comb source," *J. Opt. Commun. Netw.* **8**(2), 112–117 (2016).
15. V. Vujicic, A. Anthur, V. Panapakkam, R. Zhou, Q. Gaimard, K. Merghem, F. Lelarge, A. Ramdane, and L. Barry, "Tbit/s optical interconnects based on low linewidth quantum-dash lasers and coherent detection," in *Conference on Lasers and Electro-Optics*, OSA Technical Digest (2016), paper SF2F.4.
16. Z. Lu, J. Liu, L. Mao, C.-Y. Song, J. Weber, and P. Poole, "12.032 Tbit/s coherent transmission using an ultra-narrow linewidth quantum dot 34.46-GHz C-Band coherent comb laser," in *Next-Generation Optical Communication: Components, Sub-Systems, and Systems VIII* (Vol. 10947, p. 109470J). International Society for Optics and Photonics (2019).
17. P. Marin-Palomo, J. N. Kemal, P. Trocha, S. Wolf, K. Merghem, F. Lelarge, A. Ramdane, W. Freude, S. Randel, and C. Koos, "Comb-based WDM transmission at 10 Tbit/s using a DC-driven quantum-dash mode-locked laser diode," *Opt. Express* (2019, in Press).
18. C. Weimann, P. C. Schindler, R. Palmer, S. Wolf, D. Bekele, D. Korn, J. Pfeifle, S. Koeber, R. Schmogrow, L. Alloatti, D. Elder, H. Yu, W. Bogaerts, L. R. Dalton, W. Freude, J. Leuthold, and C. Koos, "Silicon-organic hybrid (SOH) frequency comb sources for terabit/s data transmission," *Opt. Express* **22**(3), 3629–3637 (2014).
19. J. Lin, H. Sepehrian, Y. Xu, L. A. Rusch, and W. Shi, "Frequency comb generation using a CMOS compatible SiP DD-MZM for flexible networks," *IEEE Photonics Technol. Lett.* **30**(17), 1495–1498 (2018).
20. Lumentum. Micro-Integrable Tunable Laser Assembly (ITLA), 100 kHz Linewidth, LambdaFLEX (2019). (accessed October 7, 2019). <https://www.lumentum.com/en/products/micro-itla-tunable-laser-100-khz>.
21. G. P. Agrawal, "7. Loss management," in *Fiber-Optic Communication Systems*, 4th ed. Wiley, Hoboken, NJ, USA, 2011.
22. T. J. Kippenberg, A. L. Gaeta, M. Lipson, and M. L. Gorodetsky, "Dissipative Kerr solitons in optical microresonators," *Science* **361**(6402), eaan8083 (2018).
23. R. J. Essiambre, G. Kramer, P. J. Winzer, G. J. Foschini, and B. Goebel, "Capacity limits of optical fiber networks," *J. Lightwave Technol.* **28**(4), 662–701 (2010).
24. T. Pfau, S. Hoffman, and R. Noé, "Hardware-efficient coherent digital receiver concept with feedforward carrier recovery for M-QAM constellations," *J. Lightwave Technol.* **27**(8), 989–999 (2009).
25. G. P. S. Cho, V. S. Grigoryan, Y. A. Godin, A. Salamon, and Y. Achiam, "Transmission of 25-Gb/s RZ-DQPSK signals with 25-GHz channel spacing over 1000 km of SMF-28 fiber," *IEEE Photonics Technol. Lett.* **15**(3), 473–475 (2003).
26. G. Raybon, P. J. Winzer, and C. R. Doerr, "1-Tb/s (10 × 107 Gb/s) Electronically Multiplexed Optical Signal Generation and WDM Transmission," *J. Lightwave Technol.* **25**(1), 233–238 (2007).
27. Auxora, Duplex DWDM MUX & DEMUX Module, (2018). (accessed October 11, 2019). <http://www.auxora.com/product/info2.aspx?itemid=171&lcid=45&ppid=7&pid=23>

28. Fujitsu, DP-QPSK 100G LN Modulator, (2014). (accessed January 7, 2019). <http://www.fujitsu.com/downloads/JP/archive/imgjp/group/foc/services/100gln/ln100dpqpsk-e-141105.pdf>
29. Y. Cai, W. Wang, W. Qian, J. Xing, K. Tao, J. Yin, S. Zhang, M. Lei, E. Sun, K. Yang, H. Chien, Q. Liao, and H. Chen, FPGA Investigation on Error-Floor Performance of a Concatenated Staircase and Hamming Code for 400G-ZR Forward Error Correction, in: *Opt. Fiber Commun. Conf. Postdeadline Pap.*, OSA, Washington, D.C., 2018: p. Th4C.2.
30. A. Blanco-Redondo, C. M. de Sterke, J. E. Sipe, T. F. Krauss, B. J. Eggleton, and C. Husko, "Pure-quartic solitons," *Nat. Commun.* **7**(1), 10427 (2016).
31. J. Liu, A. S. Raja, M. Karpov, B. Ghadiani, M. H. P. Pfeiffer, B. Du, N. J. Engelsen, H. Guo, M. Zervas, and T. J. Kippenberg, "Ultralow-power chip-based soliton microcombs for photonic integration," *Optica* **5**(10), 1347–1353 (2018).
32. B. Stern, X. Ji, Y. Okawachi, A. L. Gaeta, and M. Lipson, "Battery-operated integrated frequency comb generator," *Nature* **562**(7727), 401–405 (2018).
33. R. Essiambre and R. W. Tkach, "Capacity trends and limits of optical communication networks," *Proc. IEEE* **100**(5), 1035–1055 (2012).
34. Keysight Technologies, M8194A 120 GSa/s Arbitrary Waveform Generator. (accessed December 15, 2019) <https://www.keysight.com/en/pd-2951700-pn-M8194A/120-gsa-s-arbitrary-waveform-generator?cc=US&lc=eng>
35. Y. Ogiso, J. Ozaki, Y. Ueda, H. Wakita, M. Nagatani, H. Yamazaki, M. Nakamura, T. Kobayashi, S. Kanazawa, T. Fujii, Y. Hashizume, H. Tanobe, N. Nunoya, M. Ida, Y. Miyamoto, and M. Ishikawa, "Ultra-High Bandwidth InP IQ Modulator for Beyond 100-GBd transmission," in *Optical Fiber Communication Conference*, (OSA, 2019), paper M2F.2.
36. R. Dar, M. Feder, A. Mecozzi, and M. Shtaif, "Accumulation of nonlinear interference noise in fiber-optic systems," *Opt. Express* **22**(12), 14199–14211 (2014).
37. T. Akiyama, M. Ekawa, M. Sugawara, K. Kawaguchi, H. Sudo, A. Kuramata, H. Ebe, and Y. Arakawa, "An ultrawide-band semiconductor optical amplifier having an extremely high penalty-free output power of 23 dBm achieved with quantum dots," *IEEE Photonics Technol. Lett.* **17**(8), 1614–1616 (2005).